Ilkogretim Online - Elementary Education Online, 2021; Vol 20 (Issue 6): pp. 4778-4793
http://ilkogretim-online.org
doi: 10.17051/ilkonline.2021.06.465

Design And Simulation Of Optical Code Converters

Dr. A. S. Rathore Research Guide, Department of Electronics & Communication Engineering, Sri Satya Sai University of Technology & Medical Sciences, Sehore, M.P.

Arun G Research Scholar , Department of Electronics & Communication Engineering, Sri Satya Sai University of Technology & Medical Sciences, Sehore, M.P.

Dr. Sudhir N Shelke Principal, Guru Nanak Institute of Technology, Nagpur.

ABSTRACT:

The applications that need high-speed decoding/encoding, optical packet routing/switching, ultra-fast computation, and code conversion look poised to benefit from this new optical technology. There was a proposal for an optical decoder and encoder in the prior chapter. One of the benefits of signal (optical) processing is the range of analysis options it gives. It is impossible to create optical parts without optical logic gates. In this article, design and simulation of optical code converters has been discussed.

Keywords: Optical, Code, Converters, Boolean

INTRODUCTION:

The conversion from binary to octal (B-O) is seen in Figure. In this case, seven MZIs are employed to create the B-O converter. On MZI1's first input terminal, an optical CW signal is applied. Input terminal one of MZI3 and MZI2 are connected to the output terminals (1 and 2) of MZI1.

Design of Binary to Octal Code Converter:

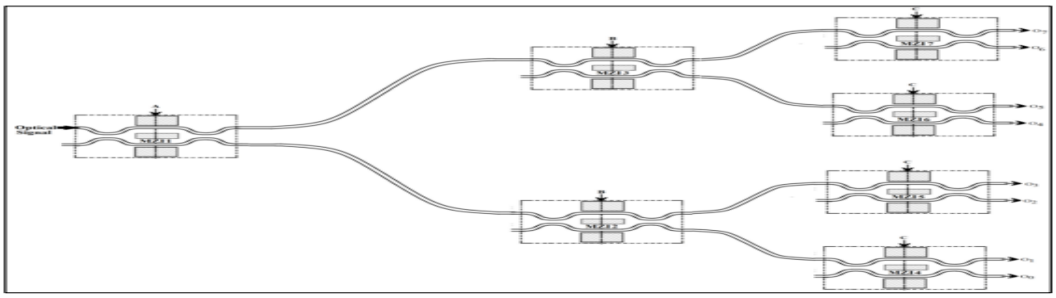

Figure 1. Conceptual diagram of binary to octal code converter using MZIs

First input terminals of MZI5 and MZI4 are connected to additional output terminals (1 and 2) of MZI2. In a similar fashion, terminal one of MZI7 is connected to the first output of MZI3, and terminal one of MZI6 is connected to the first output of MZI3. Electrode 2 of MZI1 receives the binary value A. (electrical voltage is equal to 6.75 V). Electrode 2 of MZI2 and MZI3 provides Bit B. Bit C is similarly supplied at the central electrode of MZI4, MZI5, MZI6, and MZI7. The octal outputs are considered as O_0, O_1, O_2, O_3, O_4, O_5, O_6, and O_7.

Mathematical formulation of binary to octal code converter:

Power for the B-O code converter is supplied to MZI4, MZI5, MZI6, and MZI7 through their second output terminals. Hence, the normalized power at the output terminals (O_0, O_1, O_2, O_3, O_4, O_5, O_6, and O_7) is determined by using the mathematical formula of single stage of MZI provided in Eqs (12) and (13) respectively.

The output $O0$ at output terminal two of MZI4 as;

$$O_{0_{MZI4}} = \begin{bmatrix} \left\{ je^{-j(\varphi_{oMZI_1})} \cos\left(\frac{\Delta\varphi_{MZI_1}}{2}\right)\right\} \\ \left\{ je^{-j(\varphi_{oMZI_2})} \cos\left(\frac{\Delta\varphi_{MZI_2}}{2}\right)\right\} \\ \left\{ je^{-j(\varphi_{oMZI_4})} \cos\left(\frac{\Delta\varphi_{MZI_4}}{2}\right)\right\} \end{bmatrix} E_{in}$$

$$\frac{O_{0_{MZI4}}}{E_{in}} = \begin{bmatrix} \left\{ je^{-j(\varphi_{oMZI_1})} \cos\left(\frac{\Delta\varphi_{MZI_1}}{2}\right)\right\} \\ \left\{ je^{-j(\varphi_{oMZI_2})} \cos\left(\frac{\Delta\varphi_{MZI_2}}{2}\right)\right\} \\ \left\{ je^{-j(\varphi_{oMZI_4})} \cos\left(\frac{\Delta\varphi_{MZI_4}}{2}\right)\right\} \end{bmatrix}$$

$$O_0 = \left|\frac{O_{0_{MZI4}}}{E_{in}}\right|^2 = cos^2\left(\frac{\Delta\varphi_{MZI_1}}{2}\right) cos^2\left(\frac{\Delta\varphi_{MZI_2}}{2}\right) cos^2\left(\frac{\Delta\varphi_{MZI_4}}{2}\right)$$

The first output terminal O_1 of MZI4's output is defined as;

$$O_{1_{MZI4}} = \begin{bmatrix} \left\{ je^{-j(\varphi_{oMZI_1})} \cos\left(\frac{\Delta\varphi_{MZI_1}}{2}\right)\right\} \\ \left\{ je^{-j(\varphi_{oMZI_2})} \cos\left(\frac{\Delta\varphi_{MZI_2}}{2}\right)\right\} \\ \left\{ -je^{-j(\varphi_{oMZI_4})} \sin\left(\frac{\Delta\varphi_{MZI_4}}{2}\right)\right\} \end{bmatrix} E_{in}$$

$$\frac{O_{1MZI4}}{E_{in}} = \begin{bmatrix} \left\{ je^{-j(\varphi_{oMZI1})} \cos\left(\frac{\Delta\varphi_{MZI1}}{2}\right)\right\} \\ \left\{ je^{-j(\varphi_{oMZI2})} \cos\left(\frac{\Delta\varphi_{MZI2}}{2}\right)\right\} \\ \left\{ -je^{-j(\varphi_{oMZI4})} \sin\left(\frac{\Delta\varphi_{MZI4}}{2}\right)\right\} \end{bmatrix}$$

$$O_1 = \left|\frac{O_{1MZI4}}{E_{in}}\right|^2 = cos^2\left(\frac{\Delta\varphi_{MZI1}}{2}\right) cos^2\left(\frac{\Delta\varphi_{MZI2}}{2}\right) sin^2\left(\frac{\Delta\varphi_{MZI4}}{2}\right)$$

O_2 is discharged from MZI5's second terminal as;

$$O_{2_{MZI5}} = \begin{bmatrix} \left\{ je^{-j(\varphi_{oMZI1})} \cos\left(\frac{\Delta\varphi_{MZI1}}{2}\right)\right\} \\ \left\{ -je^{-j(\varphi_{oMZI2})} \sin\left(\frac{\Delta\varphi_{MZI2}}{2}\right)\right\} \\ \left\{ je^{-j(\varphi_{oMZI5})} \cos\left(\frac{\Delta\varphi_{MZI5}}{2}\right)\right\} \end{bmatrix} E_{in}$$

$$\frac{O_{2MZI5}}{E_{in}} = \begin{bmatrix} \left\{ je^{-j(\varphi_{oMZI1})} \cos\left(\frac{\Delta\varphi_{MZI1}}{2}\right)\right\} \\ \left\{ -je^{-j(\varphi_{oMZI2})} \sin\left(\frac{\Delta\varphi_{MZI2}}{2}\right)\right\} \\ \left\{ je^{-j(\varphi_{oMZI5})} \cos\left(\frac{\Delta\varphi_{MZI5}}{2}\right)\right\} \end{bmatrix}$$

$$O_2 = \left|\frac{O_{2MZI5}}{E_{in}}\right|^2 = cos^2\left(\frac{\Delta\varphi_{MZI1}}{2}\right) sin^2\left(\frac{\Delta\varphi_{MZI2}}{2}\right) cos^2\left(\frac{\Delta\varphi_{MZI5}}{2}\right)$$

At MZI5's first output terminal, O_3 is output as;

$$O_{3_{MZI5}} = \begin{bmatrix} \left\{ je^{-j(\varphi_{oMZI1})} \cos\left(\frac{\Delta\varphi_{MZI1}}{2}\right)\right\} \\ \left\{ -je^{-j(\varphi_{oMZI2})} \sin\left(\frac{\Delta\varphi_{MZI2}}{2}\right)\right\} \\ \left\{ -je^{-j(\varphi_{oMZI5})} \sin\left(\frac{\Delta\varphi_{MZI5}}{2}\right)\right\} \end{bmatrix} E_{in}$$

$$\frac{O_{3MZI5}}{E_{in}} = \begin{bmatrix} \left\{ je^{-j(\varphi_{oMZI1})} \cos\left(\frac{\Delta\varphi_{MZI1}}{2}\right)\right\} \\ \left\{ -je^{-j(\varphi_{oMZI2})} \sin\left(\frac{\Delta\varphi_{MZI2}}{2}\right)\right\} \\ \left\{ -je^{-j(\varphi_{oMZI5})} \sin\left(\frac{\Delta\varphi_{MZI5}}{2}\right)\right\} \end{bmatrix}$$

$$O_3 = \left|\frac{O_{3MZI5}}{E_{in}}\right|^2 = cos^2\left(\frac{\Delta\varphi_{MZI1}}{2}\right) sin^2\left(\frac{\Delta\varphi_{MZI2}}{2}\right) sin^2\left(\frac{\Delta\varphi_{MZI5}}{2}\right)$$

The MZI6 output O_4 is defined as;

$$O_{4_{MZI6}} = \begin{bmatrix} \left\{-je^{-j(\varphi_{oMZI1})} \sin\left(\frac{\Delta\varphi_{MZI1}}{2}\right)\right\} \\ \left\{je^{-j(\varphi_{oMZI3})} \cos\left(\frac{\Delta\varphi_{MZI3}}{2}\right)\right\} \\ \left\{je^{-j(\varphi_{oMZI5})} \cos\left(\frac{\Delta\varphi_{MZI6}}{2}\right)\right\} \end{bmatrix} E_{in}$$

$$\frac{O_{4MZI6}}{E_{in}} = \begin{bmatrix} \left\{-je^{-j(\varphi_{oMZI1})} \sin\left(\frac{\Delta\varphi_{MZI1}}{2}\right)\right\} \\ \left\{je^{-j(\varphi_{oMZI3})} \cos\left(\frac{\Delta\varphi_{MZI3}}{2}\right)\right\} \\ \left\{je^{-j(\varphi_{oMZI5})} \cos\left(\frac{\Delta\varphi_{MZI6}}{2}\right)\right\} \end{bmatrix}$$

$$O_4 = \left|\frac{O_{4MZI6}}{E_{in}}\right|^2 = sin^2\left(\frac{\Delta\varphi_{MZI1}}{2}\right) cos^2\left(\frac{\Delta\varphi_{MZI3}}{2}\right) cos^2\left(\frac{\Delta\varphi_{MZI6}}{2}\right)$$

O_5 is the signal at MZI6's first output terminal.

$$O_{5_{MZI6}} = \begin{bmatrix} \left\{-je^{-j(\varphi_{oMZI1})} \sin\left(\frac{\Delta\varphi_{MZI1}}{2}\right)\right\} \\ \left\{je^{-j(\varphi_{oMZI3})} \cos\left(\frac{\Delta\varphi_{MZI3}}{2}\right)\right\} \\ \left\{-je^{-j(\varphi_{oMZI6})} \sin\left(\frac{\Delta\varphi_{MZI6}}{2}\right)\right\} \end{bmatrix} E_{in}$$

$$\frac{O_{5MZI6}}{E_{in}} = \begin{bmatrix} \left\{-je^{-j(\varphi_{oMZI1})} \sin\left(\frac{\Delta\varphi_{MZI1}}{2}\right)\right\} \\ \left\{je^{-j(\varphi_{oMZI3})} \cos\left(\frac{\Delta\varphi_{MZI3}}{2}\right)\right\} \\ \left\{-je^{-j(\varphi_{oMZI6})} \sin\left(\frac{\Delta\varphi_{MZI6}}{2}\right)\right\} \end{bmatrix}$$

$$O_5 = \left|\frac{O_{5MZI6}}{E_{in}}\right|^2 = sin^2\left(\frac{\Delta\varphi_{MZI1}}{2}\right) cos^2\left(\frac{\Delta\varphi_{MZI3}}{2}\right) sin^2\left(\frac{\Delta\varphi_{MZI6}}{2}\right)$$

This is the result of MZI7's second output terminal's O_6 signal being interpreted as;

$$O_{6_{MZI7}} = \begin{bmatrix} \left\{-je^{-j(\varphi_{oMZI_1})}\sin\left(\frac{\Delta\varphi_{MZI_1}}{2}\right)\right\} \\ \left\{-je^{-j(\varphi_{oMZI_8})}\sin\left(\frac{\Delta\varphi_{MZI_8}}{2}\right)\right\} \\ \left\{je^{-j(\varphi_{oMZI_7})}\cos\left(\frac{\Delta\varphi_{MZI_7}}{2}\right)\right\} \end{bmatrix} E_{in}$$

$$\frac{O_{6MZI7}}{E_{in}} = \begin{bmatrix} \left\{-je^{-j(\varphi_{oMZI_1})}\sin\left(\frac{\Delta\varphi_{MZI_1}}{2}\right)\right\} \\ \left\{-je^{-j(\varphi_{oMZI_8})}\sin\left(\frac{\Delta\varphi_{MZI_8}}{2}\right)\right\} \\ \left\{je^{-j(\varphi_{oMZI_7})}\cos\left(\frac{\Delta\varphi_{MZI_7}}{2}\right)\right\} \end{bmatrix}$$

$$O_6 = \left|\frac{O_{6MZI7}}{E_{in}}\right|^2 = sin^2\left(\frac{\Delta\varphi_{MZI_1}}{2}\right) sin^2\left(\frac{\Delta\varphi_{MZI_8}}{2}\right) cos^2\left(\frac{\Delta\varphi_{MZI_7}}{2}\right)$$

Input terminal one of MZI7 produces O_6 as an output;

$$O_{7_{MZI7}} = \begin{bmatrix} \left\{-je^{-j(\varphi_{oMZI_1})}\sin\left(\frac{\Delta\varphi_{MZI_1}}{2}\right)\right\} \\ \left\{-je^{-j(\varphi_{oMZI_8})}\sin\left(\frac{\Delta\varphi_{MZI_8}}{2}\right)\right\} \\ \left\{-je^{-j(\varphi_{oMZI_7})}\sin\left(\frac{\Delta\varphi_{MZI_7}}{2}\right)\right\} \end{bmatrix} E_{in}$$

$$\frac{O_{7MZI7}}{E_{in}} = \begin{bmatrix} \left\{-je^{-j(\varphi_{oMZI_1})}\sin\left(\frac{\Delta\varphi_{MZI_1}}{2}\right)\right\} \\ \left\{-je^{-j(\varphi_{oMZI_8})}\sin\left(\frac{\Delta\varphi_{MZI_8}}{2}\right)\right\} \\ \left\{-je^{-j(\varphi_{oMZI_7})}\sin\left(\frac{\Delta\varphi_{MZI_7}}{2}\right)\right\} \end{bmatrix}$$

$$O_7 = \left|\frac{O_{7MZI7}}{E_{in}}\right|^2 = sin^2\left(\frac{\Delta\varphi_{MZI_1}}{2}\right) sin^2\left(\frac{\Delta\varphi_{MZI_8}}{2}\right) sin^2\left(\frac{\Delta\varphi_{MZI_7}}{2}\right)$$

The equation for determining the phase difference in MZI is $\Delta\varphi MZI1 = \varphi 11 - \varphi 12$, $\varphi_{11} = \frac{\pi}{V\pi}A$, $\varphi_{12} = \frac{\pi}{V\pi}B$, where, $A = 6.75V$ and $B = 0V$. Similarly, the phase difference of any MZI may be determined.

As shown in Figures, the B-O code converter's simulation results in MATLAB vary depending on the control signals used '*ABC*' (*i. e* 000, 001, 010, ……, 111). The output O_0 is obtained at control signal $A = 0$, $B = 0$ and $C = 0$. Similarly, output O_1, O_2, …… O_7, produced by varying the control signals as described in Table. The signals *A*, *B* and *C* may be seen in the first, second, and third columns, respectively. Octal values are displayed in the last column.

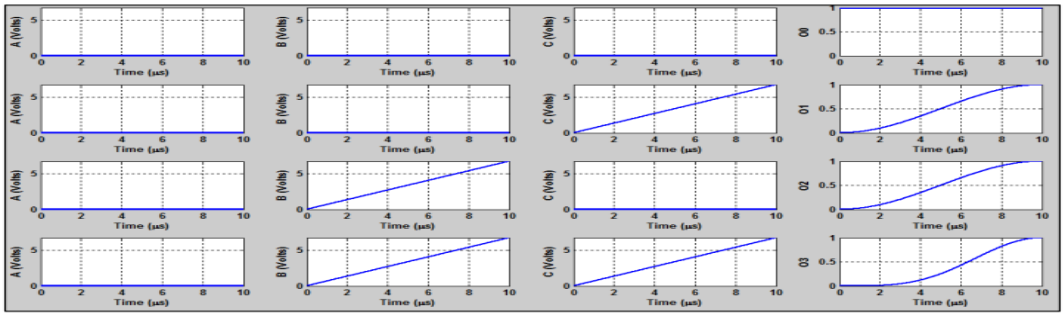

(a)

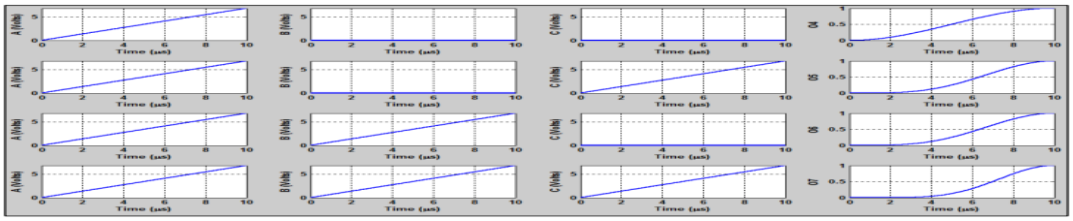

(b)

Figure 2. MATLAB simulation result for □□□ (a): 000 to 011 (b): 100 to 111 of B-O code converter

Table 1. Truth table of binary to octal code converter using MZIs

Binary input			Octal Output							
A	B	C	O_0	O_1	O_2	O_3	O_4	O_5	O_6	O_7
0	0	0	1	0	0	0	0	0	0	0
0	0	1	0	1	0	0	0	0	0	0
0	1	0	0	0	1	0	0	0	0	0
0	1	1	0	0	0	1	0	0	0	0
1	0	0	0	0	0	0	1	0	0	0
1	0	1	0	0	0	0	0	1	0	0
1	1	0	0	0	0	0	0	0	1	0
1	1	1	0	0	0	0	0	0	0	1

Simulation results and discussion of binary to octal code converter using BPM:

In Figure, we see the BPM architecture for the transformation of binary to octal. The circuitry employed here makes use of seven MZIs. The first input terminal of MZI1 receives an optical signal. The first input terminals of MZI2 and MZI3 are connected to the first output terminals of MZI1. One input terminal from MZI4, MZI5, MZI6, and MZI7 is connected to their respective output terminals. Electrical signals carrying the control signals (A, B and C) are encoded using binary bits. Figure depicts where the three control signals (A, B and C) should be in relation to the various MZIs.

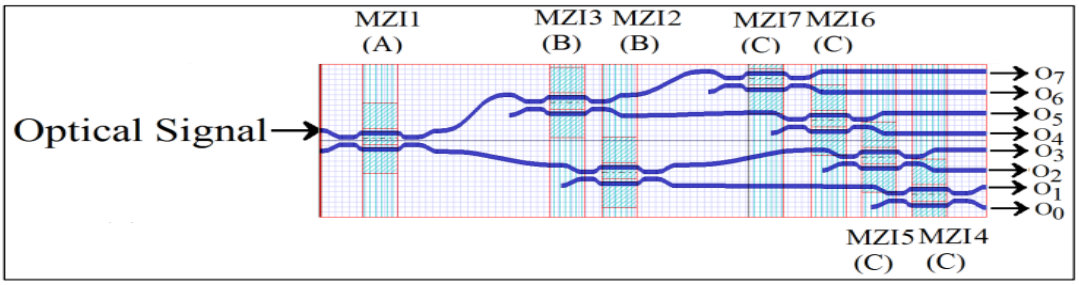

Figure 3. Design of binary to octal code converter

By applying inputs (A, B, C) to the central electrode in various orders, the resulting responses are detailed below:

Case 1: □ = 0, □ = 0, □ = 0

In this case, the optical input signal is fed into MZI1's first input; then, with the control signal A = 0, the optical output signal is sent out MZI1's second terminal. The first input terminal of MZI2 is connected to this terminal. When B is zero, MZI2's second output terminal, which is connected to MZI4's first input terminal, becomes active and emits an optical signal. Now that we know that, when C = 0, the signal is produced at terminal two of MZI4 (0_0 = 1).

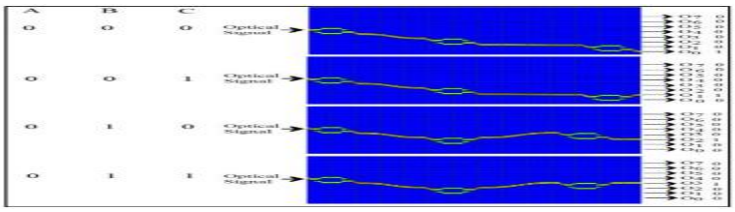

(a)

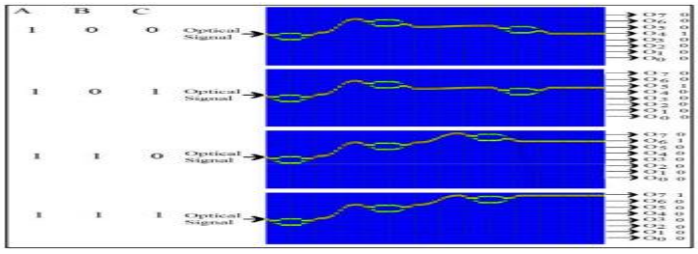

(b)

Figure 4. Results of binary to octal code converter for different combinations of control signals (a): □□□ = 000 to 011 (b): □□□ = 100 to 111 obtained through beam propagation method

Case 2: □ = 0, □ = 0, □ = 1

Control signals, A = 0, and B = 0, the signal (optical), again emerge at MZI2's second output terminal. Having set C = 1, the optical signal is now being transmitted out of MZI4's terminal 1, or 0_1 = 1.

Case 3: □ = 0, □ = 1, □ = 0

In this situation, however, the control signal is A = 0, while B = 1. This means that the optical signal coming from terminal two of MZI1 will be fed into MZI2's terminal 1 for processing, and since B = 1, the optical signal will then be output from terminal 1 of MZI2. In the absence of current, a signal (optical) is produced at terminal two of MZI5 as C = 0, i.e.0_2 = 1.

Case 4: □ = 0, □ = 1, □ = 1

Similar to the previous example, the control signals A = 0 and B = 1 the signal (optical) arrive at MZI2's first output terminal. Now, in this example, C = 1, the optical signal is produced at MZI5's first output terminal i.e.0_3 = 1.

Case 5: □ = 1, □ = 0, □ = 0

Since the control signal, A = 1, causes the signal (optical) to emerge at MZI1's output terminal 1, this instance is distinct from all the others. At B = 0, the second MZI3 output terminal begins to receive an optical signal. These wires connect to MZI6's primary input. When C is set to zero, MZI6's output emerges at its second terminal i.e. 0_4 = 1.

Case 6: □ = 1, □ = 0, □ = 1

Similar to the previous example, the signal (optical) occurs at MZI3's second output terminal when the control signals, A = 1 and B = 0. When C set to 1, MZI6's first terminal is now the output i.e.0_5 = 1.

Case 7: □ = 1, □ = 1, □ = 0

At MZI3's first output terminal, we see both the initial control signals, A = 1 and B = 1 (optical). Now that C = 0, we see the output coming out of MZI7's second terminal i.e.0_6 = 1.

Case 8: □ = 1, □ = 1, □ = 1

In this situation, everything is reversed from the previous examples; the control signals (A = 1, B = 1, C = 1) for the optical signal will arrive at the first output terminal of MZI7, making 0_7 = 1. In Figures, we see the truth table in Table being used to verify the aforementioned scenarios.

Design of Octal To Binary Code Converter:

The conversion diagram from octal to binary (O-B) is shown in Figure. Eight MZIs were used in the design of this. The Octal numeral system uses the numbers 0 through 7. In this case, these numbers are written as $I0$, $I1$…..$I7$.

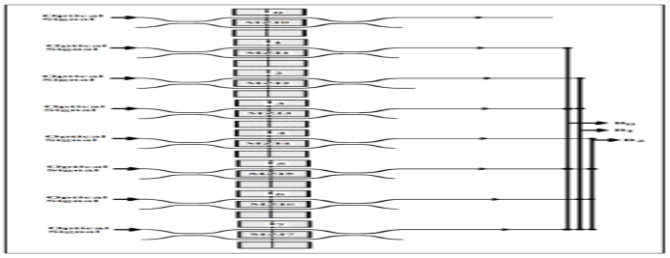

Figure 5. Conceptual diagram of octal to binary code converter

Octal bits I_0, I_1, I_2, I_3, I_4, I_5, I_6, and I_7 are delivered at electrode two of MZI0, MZI1, MZI2, MZI3, MZI4, MZI5, MZI6, and MZI7. Bit B_0 in the binary representation is the result of adding the signals at the first output terminal of MZI1, MZI3, MZI5, and MZI7. Like MZI1, the first terminal of MZI2, MZI3, MZI6, and MZI7 are combined to form B_1. Bit B_2 of the binary representation is the aggregate value of the first terminal outputs of MZI4, MZI5, MZI6, and MZI7. At electrode two of the MZI0 to MZI7, a control signal (electrical signal with potential 6.75 V) is delivered to initiate the code conversion with its eight inputs (I_0, I_1…..I_7) and three binary (B_0, B_1 and B_2) outputs, the O-B code converter is a code translator. The truth table for the octal to binary code converter is displayed in Table.

Table 2. Truth table of octal to binary code converter

Octal Input								Binary output		
I_0	I_1	I_2	I_3	I_4	I_5	I_6	I_7	B_2	B_1	B_0
1	0	0	0	0	0	0	0	0	0	0
0	1	0	0	0	0	0	0	0	0	1
0	0	1	0	0	0	0	0	0	1	0
0	0	0	1	0	0	0	0	0	1	1
0	0	0	0	1	0	0	0	1	0	0
0	0	0	0	0	1	0	0	1	0	1
0	0	0	0	0	0	1	0	1	1	0
0	0	0	0	0	0	0	1	1	1	1

Mathematical formulation of octal to binary code converter:

To activate the O-B code converter, current must now be supplied to one of the terminals labelled MZI0, MZI1, MZI2, MZI3, MZI4, MZI5, MZI6, or MZI7. Normalized powers at the output terminals (B_0, B_1 and B_2) are computed to show the operation of the O-B code converter analytically. The normalized output power is calculated using the single-stage MZI mathematical formula in Eqs. (12) and (13). The resulting result, B_0, is the output;

$$B_0 = \begin{bmatrix} \left\{-je^{-j(\varphi_{oMZI_1})}\sin\left(\frac{\Delta\varphi_{MZI_1}}{2}\right)\right\} \\ \left\{-je^{-j(\varphi_{oMZI_3})}\sin\left(\frac{\Delta\varphi_{MZI_3}}{2}\right)\right\} \\ \left\{-je^{-j(\varphi_{oMZI_5})}\sin\left(\frac{\Delta\varphi_{MZI_5}}{2}\right)\right\} \\ \left\{-je^{-j(\varphi_{oMZI_7})}\sin\left(\frac{\Delta\varphi_{MZI_7}}{2}\right)\right\} \end{bmatrix} E_{in}$$

$$\frac{B_0}{E_{in}} = \begin{bmatrix} \left\{-je^{-j(\varphi_{oMZI_1})}\sin\left(\frac{\Delta\varphi_{MZI_1}}{2}\right)\right\} \\ \left\{-je^{-j(\varphi_{oMZI_3})}\sin\left(\frac{\Delta\varphi_{MZI_3}}{2}\right)\right\} \\ \left\{-je^{-j(\varphi_{oMZI_5})}\sin\left(\frac{\Delta\varphi_{MZI_5}}{2}\right)\right\} \\ \left\{-je^{-j(\varphi_{oMZI_7})}\sin\left(\frac{\Delta\varphi_{MZI_7}}{2}\right)\right\} \end{bmatrix} E_{in}$$

$$B_0 = \left|\frac{B_0}{E_{in}}\right|^2 = sin^2\left(\frac{\Delta\varphi_{MZI_1}}{2}\right) + sin^2\left(\frac{\Delta\varphi_{MZI_3}}{2}\right) + sin^2\left(\frac{\Delta\varphi_{MZI_5}}{2}\right) + sin^2\left(\frac{\Delta\varphi_{MZI_7}}{2}\right)$$

The obtained output B_1 is shown here;

$$B_1 = \begin{bmatrix} \left\{-je^{-j(\varphi_{oMZI_2})}\sin\left(\frac{\Delta\varphi_{MZI_2}}{2}\right)\right\} \\ \left\{-je^{-j(\varphi_{oMZI_3})}\sin\left(\frac{\Delta\varphi_{MZI_3}}{2}\right)\right\} \\ \left\{-je^{-j(\varphi_{oMZI_6})}\sin\left(\frac{\Delta\varphi_{MZI_6}}{2}\right)\right\} \\ \left\{-je^{-j(\varphi_{oMZI_7})}\sin\left(\frac{\Delta\varphi_{MZI_7}}{2}\right)\right\} \end{bmatrix} E_{in}$$

$$\frac{B_1}{E_{in}} = \begin{bmatrix} \left\{-je^{-j(\varphi_{oMZI_2})}\sin\left(\frac{\Delta\varphi_{MZI_2}}{2}\right)\right\} \\ \left\{-je^{-j(\varphi_{oMZI_3})}\sin\left(\frac{\Delta\varphi_{MZI_3}}{2}\right)\right\} \\ \left\{-je^{-j(\varphi_{oMZI_6})}\sin\left(\frac{\Delta\varphi_{MZI_6}}{2}\right)\right\} \\ \left\{-je^{-j(\varphi_{oMZI_7})}\sin\left(\frac{\Delta\varphi_{MZI_7}}{2}\right)\right\} \end{bmatrix}$$

$$B_1 = \left|\frac{B_1}{E_{in}}\right|^2 = sin^2\left(\frac{\Delta\varphi_{MZI_2}}{2}\right) + sin^2\left(\frac{\Delta\varphi_{MZI_3}}{2}\right) + sin^2\left(\frac{\Delta\varphi_{MZI_6}}{2}\right) + sin^2\left(\frac{\Delta\varphi_{MZI_7}}{2}\right)$$

The obtained output B_2 is shown here;

$$B_2 = \begin{bmatrix} \left\{-je^{-j(\varphi_{0MZI4})}\sin\left(\frac{\Delta\varphi_{MZI4}}{2}\right)\right\} \\ \left\{-je^{-j(\varphi_{0MZI5})}\sin\left(\frac{\Delta\varphi_{MZI5}}{2}\right)\right\} \\ \left\{-je^{-j(\varphi_{0MZI6})}\sin\left(\frac{\Delta\varphi_{MZI6}}{2}\right)\right\} \\ \left\{-je^{-j(\varphi_{0MZI7})}\sin\left(\frac{\Delta\varphi_{MZI7}}{2}\right)\right\} \end{bmatrix} E_{in}$$

$$\frac{B_2}{E_{in}} = \begin{bmatrix} \left\{-je^{-j(\varphi_{0MZI4})}\sin\left(\frac{\Delta\varphi_{MZI4}}{2}\right)\right\} \\ \left\{-je^{-j(\varphi_{0MZI5})}\sin\left(\frac{\Delta\varphi_{MZI5}}{2}\right)\right\} \\ \left\{-je^{-j(\varphi_{0MZI6})}\sin\left(\frac{\Delta\varphi_{MZI6}}{2}\right)\right\} \\ \left\{-je^{-j(\varphi_{0MZI7})}\sin\left(\frac{\Delta\varphi_{MZI7}}{2}\right)\right\} \end{bmatrix}$$

$$B_2 = \left|\frac{B_2}{E_{in}}\right|^2 = sin^2\left(\frac{\Delta\varphi_{MZI4}}{2}\right) + sin^2\left(\frac{\Delta\varphi_{MZI5}}{2}\right) + sin^2\left(\frac{\Delta\varphi_{MZI6}}{2}\right) + sin^2\left(\frac{\Delta\varphi_{MZI7}}{2}\right)$$

The O-B code converter simulation results for different combinations of control signals '$I_0 to I_7$' are displayed in Figure (equivalent to octal digit 0 to 7 respectively). At control signal $I_0 = 0$, we get $B_0B_1B_2 = 000$ as an output. Similarly, Table displays the output received with various configurations of control signals. The signals $I_0 – I_7$ are shown in the first column. Bits $B_0B_1B_2$ are shown in the last column as a binary representation.

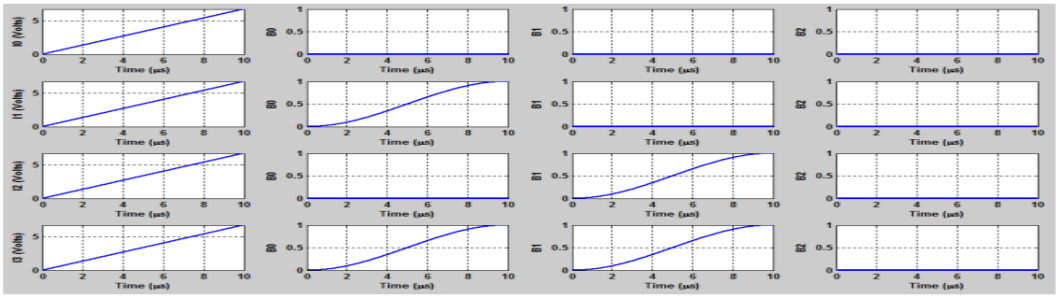

(a)

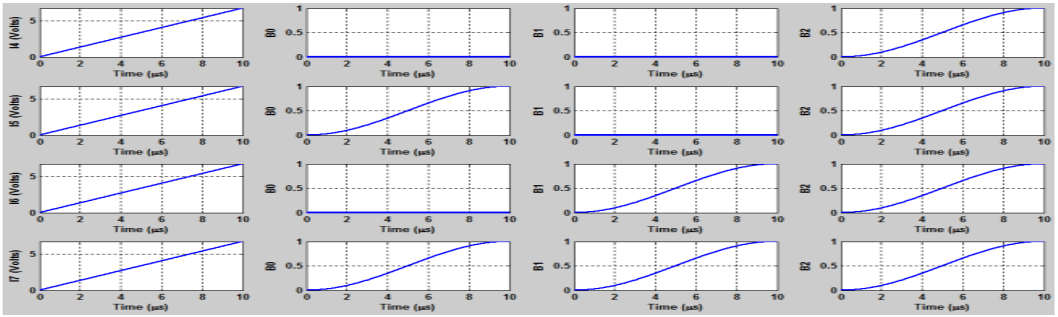

(b)

Figure 6. MATLAB simulation result for octal input (a): 0 to 3 (b): 4 to 7

Design of octal to binary code converter:

This octal to binary converter is seen in Figure. Eight MZIs are utilized in the construction of this circuit. Every one of the input terminals labelled MZI0, MZI1, MZI2, MZI3, MZI4, MZI5, MZI6, or MZI7 receives a continuous signal (optical). One of the output terminals of MZI1, MZI3, MZI5, and MZI7 are all connected to one another, and this configuration is treated as binary bit B_0. Binary bit B_1 is connected to the first output terminal of MZI2, MZI3, MZI6, and MZI7. Similarly, the first output terminal of MZI4, MZI5, MZI6, and MZI7 are combined into a single binary bit B_2.

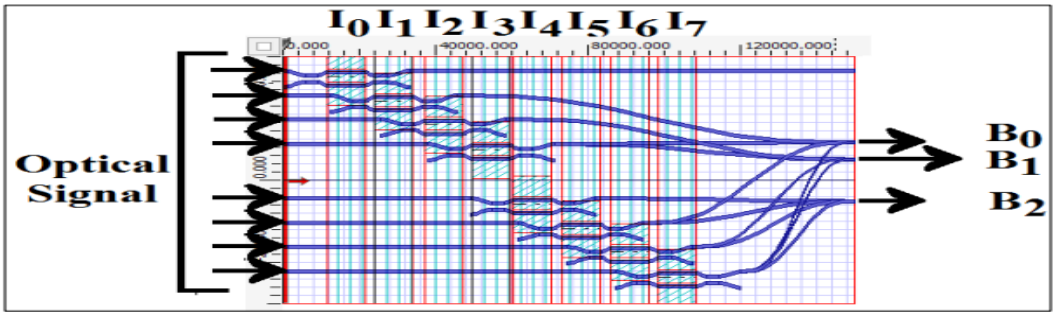

Figure 7. design of octal to binary code converter

Octal inputs I_0, I_1, I_2, I_3, I_4, I_5, I_6, I_7 are applied to electrode two of MZI0, MZI1, MZI2, MZI3, MZI4, MZI5, and MZI6. Octal to binary code conversion is explained in the following examples (Figure):

Case 1 I_0 = 1

As I_0 = 1 in octal form, a high voltage is being delivered to electrode two of MZI0. MZI0's initial output is an optical signal. Bits B_0, B_1, B_2i.e.B_0, B_1, B_2 = 000 on the output are not linked to this terminal (Figure).

Case 2 I_1 = 1

The octal input I_1 is high in this scenario. MZI1's second signal output terminal receives the optical signal. 001 indicates that this terminal is connected to the binary value of bit B_0 and that bits B_2 and B_1 both have a value of zero. The octal equivalent of the control signal for all MZIs outside MZI1 is 0. As a result of the optical signal being absorbed by the crystal (Figure).

Case 3 I_2 = 1

High values of I_2 cause MZI2's first output terminal to receive an optical signal. This terminal corresponds to binary bit B_1, while bits B_0 and B_2 are both set to zero (or 010) (Figure).

Case 4 I_3 = 1

In this case, the optical signal is obtained at MZI3's first output terminal, I_3 = 1. This terminal connects to the binary digits B_0, B_1, whereas the output from bit B_2 is zero. Hence, the octal representation of the number I_3 is 011 (Figure).

Case 5 I_4 = 1

In this situation, the first terminal of MZI4's output is active since the octal digit I_4 is high. Bit B_2 is connected to this terminal, making it logically one. $B_2B_1B_0$ = 100 indicates that bits B_0 and B_1 are both 0 (Figure).

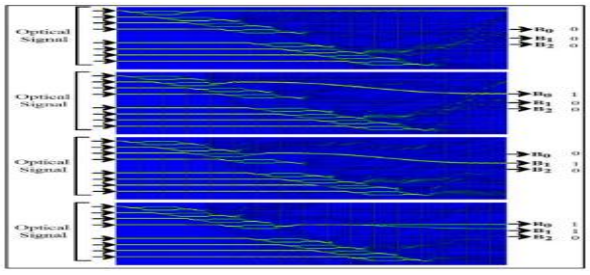

(a)

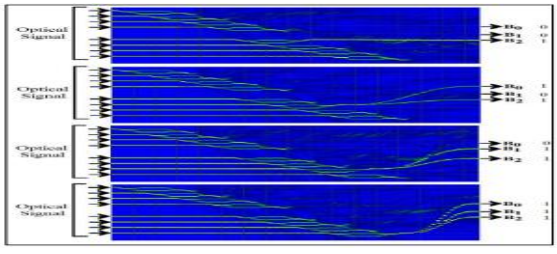

(b)

Figure 8. BPM simulation results for octal to binary code conversion from (a): 0 to 4790 | Dr. A. S. Rathore Design And Simulation Of Optical Code Converters

□3 (b): □4 to □7

Case 6 □5 = 1

In this scenario, the optical signal is obtained from MZI5's first output terminal, shown by the octal value I_5 = 1. MZI5 has its output wire connected to the binary digits B_2 and B_0. For this reason, bits B_2 and B_0 are assigned the logic 1 value, whereas bit B_1 is assigned the logic 0 value, or 101 (Figure).

Case 7 □6 = 1

Given that I_6 = 1, the MZI6 control signal is active in this case. Because of this (optical) signal, MZI6's first output is obtained. The binary digits B_2 and B_1 are connected to this terminal, therefore $B_2B_1B_0$ = 110 (Figure).

Case 8 □7 = 1

When MZI7 receives the control signal I_7 = 1, the output is sent to terminal one of the device. In binary, bit $B_2B_1B_0$ is equal to 111, hence this terminal is tied to that bit. This represents the octal value 7 (I_7) in binary.

Result and Discussion:

Both the ER and IL for the B-O code converter and the O-B code converter have been determined and are presented in Tables.

Table 3.Performance parameters for B-O converter

P^1_{min}	P^0_{max}	ER (dB)
0.9928	0.021	16.7464
P_{in}	P_{out}	IL (dB)
0.9999	0.9928	0.03095

Table 4. Performance parameters for O-B converter

P^1_{min}	P^0_{max}	ER (dB)
0.7211	0.021	15.3577
P_{in}	P_{out}	IL (dB)
0.9999	0.7211	1.41961

Both the binary to octal and the octal to binary electro-optical code converters are discussed in depth in this chapter. Electro-optical code converters like this have applications in optical

computing and data processing. The guidelines for implementing MZI-based code converters between B and O and O and B are clearly laid forth. The findings and discussion section includes the computation of several relevant parameters for an optical communication system, such as the extinction ratio and the insertion loss, as well as their subsequent discussion. Both the B-O and O-B converter ER values were estimated to be 16.7464 and 15.3577 dB.

CONCLUSION:

For this identical device, we may determine an insertion loss of 0.03095 and 1.41961 dB, respectively. Our device design hypothesis was supported by the analyzed mathematical data and the simulated outcomes generated in MATLAB. In addition, the Opti-BPM simulation programme was used to verify the described approach of implementing these devices through the finite difference beam propagation method.

REFERENCES:

A. Witkowska, S. G. Leon-Saval, A. Pham, and T. A. Birks, "All-fiber LP11 mode converters," Opt. Lett. 33, 306–308 (2008).

Chen, Kai & Li, Xue & Zheng, Yan & Chiang, Kin. (2015). Lithium-Niobate Mach-Zehnder Interferometer with Enhanced Index Contrast by SiO2 Film. Photonics Technology Letters, IEEE. 27. 1224-1227. 10.1109/LPT.2015.2415038.

H. Sakata, H. Sano, and T. Harada, "Tunable mode converter using electromagnet-induced long-period grating in two-mode fiber," Opt. Fiber Technol. 20, 224–227 (2014).

G. F. Li, N. Bai, N. B. Zhao, and C. Xia, "Space-division multiplexing: the next frontier in optical communication," Adv. Opt. Photon. 6, 413– 487 (2014).

J. D. Love and N. Riesen, "Single-, few, and multimode Y-junctions," J. Lightwave Technol. 30, 304–309 (2012).

M. Nakamura, M. Sekita, S. Takekawa and K. Kitamura, "Crystal growth and characterization of Nd, Mg co-doped near-stoichiometric LiNbO3," J. Cryst. Growth 290(1), 144-148 (2006).

N. G. Broderick, G. W. Ross, H. L. Offerhaus, D. J. Richardson and D. C. Hanna, "Hexagonally domain inverted lithium niobate: a two-dimensional nonlinear photonic crystal," Phys. Rev. Lett. 84(19), 4345–4348 (2000).

Pal, Amrindra & Kumar, Santosh & Sharma, Sandeep. (2017). Design of Optical SR Latch and Flip-Flop Using Electro-Optic Effect Inside Lithium–Niobate-Based Mach–Zehnder Interferometers. Journal of Optical Communications. 40. 10.1515/joc-2017-0053.

R. Das, S. Ghosh and R. Chakraborty, “Dependence of effective internal field of congruent lithium niobate on its domain configuration and stability”, J. Appl. Phys. 115(24), 243101 (2014).

Sergey & Suche, Hubertus & Nouroozi, Rahman & Min, Yoohong. (2008). Integrated Optical Devices in Lithium Niobate. Optics and Photonics News. 19. 24-31. 10.1364/OPN.19.1.000024.

W. Jin and K.S. Chiang,“Mode switch based on electro-optic long-period waveguide grating in lithium niobate,” Opt. Lett. 40, 237–240 (2015).

Zhang, H., Liang, C., Liu, J., Tian, Z., Wang, G. and Cai, W.,“Defect-Mediated Formation of Ag Cluster-Doped TiO2 Nanoparticles for Efficient Photodegradation of Pentachlorophenol,” Langmuir, 28, 3938–3944 (2012).